Synthesis of TiO$_2$ nantubes coupled with α-Fe$_2$O$_3$ nanoparticles and investigation of their photoelectrochemical activity

*Aiming Mao[1], Jong Hyeok Park[2], **Gui Young Han[3]

Synthesis of TiO$_2$ nantubes coupled with α-Fe$_2$O$_3$ nanoparticles and investigation of their photoelectrochemical activity

Aiming Mao, Jong Hyeok Park, Gui Young Han

Key words : Water splitting; TiO$_2$ nanotube; Hydrogen; Photoanode

Abstract : TiO$_2$ nanotube arraysdecorated with α-Fe$_2$O$_3$ were prepared by forming a nanotube-like TiO$_2$ film on a Ti sheet using an anodization process, followed by electrochemical deposition treatment to decorate hematite (α-Fe$_2$O$_3$) nanoparticles on the TiO$_2$ nanotube arrays. The SEM and XRD results revealed that the α-Fe$_2$O$_3$ nanoparticles were homogeneously embedded on the surface of the TiO$_2$ nanotube arrays. The activity of hydrogen production by photocatalytic water decomposition for the α-Fe$_2$O$_3$/TiO$_2$ nanotube array composite was examined under visible light irradiation.

1. Introduction

Water photolysis is the ideal technology for human beings to use in the future because of its advantages of the direct usage of sunlight and water and virtually unlimited resources. Especially, water decomposition technology with photocatalysts consisting of titanium oxide (TiO$_2$) has great potential to produce low priced and environmentally friendly hydrogen in the future [1-5]. Titanium oxide (TiO$_2$) nanotubes have been extensively investigated due to their distinctive one-dimensional nanostructure, which renders them useful for applications in the areas of solar cells and photocatalysis [6]. Attempts have been made to develop a hydrothermal method for the synthesis of TiO$_2$ nanotube arrays [7-12] To extend their light response region, some authors reported the successful photosensitization of TiO$_2$ nanotube arrays by coupling them with other small band gap semiconductor materials, such as CdS, ZnO and CuAlO$_2$ [13-16].

Herein, we report a simple two-step electrochemical route for the direct formation of an α-Fe$_2$O$_3$/TiO$_2$ nanotube array composite. This is a simple and efficient approach to synthesize a composite consisting of TiO$_2$ nanotube arrays loaded with α-Fe$_2$O$_3$ nanoparticles. Coupling the TiO$_2$ nanotube arrays with α-Fe$_2$O$_3$ (2.1 eV) nanoparticles, a narrow band gap semiconductor, makes it possible to extend their optical response from the UV to the visible region and improve their visible light activity. Meanwhile, the heterostructure generated at the interface between the TiO$_2$ nanotube arrays and α-Fe$_2$O$_3$ is beneficial to enhance the separation efficiency of the photogenerated electron-hole pairs. To explore the application of this new material, the α-Fe$_2$O$_3$/TiO$_2$ nanotube array composite is primarily employed as a photoanode material of photoelectrochemical cells for the production of hydrogen by photocatalytic water decomposition under visible light irradiation.

1) 성균관대학교
   E-mail : zidou1984@hotmail.com
   Tel : (031) 290-7269 Fax : (031) 290-7272
2) 성균관대학교
   E-mail : lutts@skku.edu
   Tel : (031) 290-7346 Fax : (031) 290-7346
3) 성균관대학교
   E-mail : gyhan@skku.ac.kr
   Tel : (031) 290-7249 Fax : (031) 290-7272

2. Experimental

2.1 Preparation of titanium oxide nanotube arrays

Titanium foils (0.25thick, 99.5% pure) were purchased from Alfa Aesar (Ward Hill, MA). TiO_2 nanotubes were prepared in an aqueous solution made by mixing acetic acid (CH_3COOH (99%, Daejung, Seoul, South Korea)) and 0.5hydrofluoric acid (HF (50%, J.T. Baker)) at a concentration ratio of 1:7. The electrochemical experiments were conducted using a direct current (dc) power supply (VUPOWER AK-6003). A titanium sheet served as the anodic electrode and a platinum electrode as the counter electrode. The samples were anodized at 20V (15°C) for 3 hours. After anodization, they were immediately rinsed with distilled water and then dried in an N_2 stream. They were annealed at 400°C for 6 hours with heating and cooling rates of 10°C min^{-1} in an O_2 atmosphere to crystallize the tube walls and improve the stoichiometry.

2.2 Synthesis of α-Fe₂O₃/TiO₂ nanotube array composite

Iron oxide nanoparticles were electrochemically grown by potential cycling (to deposit iron oxide?) onto TiO_2 nanotube arrays substrates. A typical three electrode electrochemical cell geometry was used, comprising a Ti foil containing the TiO_2 nanotube arrays as the working electrode, a Pt mesh as the counter electrode, and Hg/HgO as the reference electrode. The electrodeposition bath consisted of an aqueous solution of 5 mM $FeCl_3$ + 5 mM KF + 1 M H_2O_2 + 0.1 M KCl. All of the solutions were prepared from analytical-grade reagents. Electrochemical growth was done by a potential cycling procedure at a potential sweep rate of 0.02 V/s, from -0.8 V to 0.4 V vs. Hg/HgO, for a total of 10 or 20 cycles. Then, the samples were annealed in air for 1 hour at 520 ℃.

3. Results and Discussion

3.1 TiO₂ nanotube arrays

Figure 1 (a) and (b) show the scanning electron microscopy images (SEM) of the surface of the self-organized TiO_2 nanotube array layers and the side-view of the TiO_2 nanotube array, respectively. These results show that the TiO_2 nanotubes are well organized vertically and that the layer thickness is approximately 450nm after 1 hour of anodization.


(a)　　　　　　　　(b)
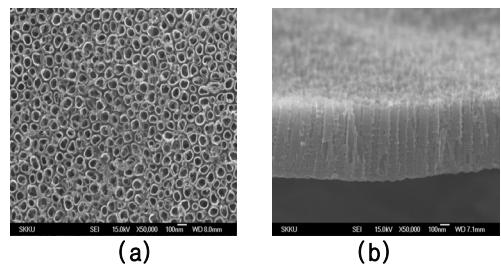
Fig. 1 FE-SEM images of TiO₂ nanotube arrays

The overall mechanism of the anodic formation of straight nanoporous titania can be represented as follows:

$$2H_2O \rightarrow O_2 + 4e^- + 4H^+ \tag{1}$$
$$Ti + O_2 \rightarrow TiO_2 \tag{2}$$
$$TiO_2 + 6F^- + 4H^+ \rightarrow TiF_6^{2-} + 2H_2O \tag{3}$$
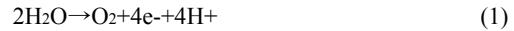
With the onset of anodization, a thin layer of oxide forms on the titanium surface. Small pits originate in this oxide layer due to the localized dissolution of the oxide, making the barrier layer at the bottom of the pits relatively thin, which, in turn, increases the electric-field intensity across the remaining barrier layer, resulting in further pore growth. The entrance to the pores is not affected by the electric-field-assisted dissolution and, hence, remains relatively narrow, while the electric field distribution in the curved bottom surface of the pores causes the widening, as well as the deepening, of the pores. This results in pores with a scallop shape [17-18]. As the Ti‑O bond energy is high (323 kJ/mol), in the case of titania, it is reasonable to assume that only pores having thin walls will be formed, due to the relatively low ion mobility and relatively high chemical solubility of the oxide in the electrolyte and, hence, unanodized metallic portions can initially exist between the pores. As the pores become deeper, the electric field in these protruded metallic regions increases, thereby enhancing the field-assisted oxide growth and oxide dissolution and, simultaneously with the pores, well-defined interpore voids start to form. Thereafter, both the voids and tubes grow in equilibrium to finally yield a tubular structure [19-20].

3.2 Deposition of α-Fe₂O₃ nanoparticles into TiO₂ Nanotube arrays

Cyclic voltammetric experiments were performed in the potential range between -1.0V and 1.0V, where the reduction of the metal precursor can be observed. Figure 2 shows the experiment result, in which the reaction voltage range can be determined, viz. from -0.8V to 0.4V. After 10 potential cycles, a red film covering the electrode surface can be observed. The X-ray Diffraction (XRD) measurements showed that a crystallite sized α-Fe₂O₃ phase was formed after calcination at 520 ℃ for 1 hour in air. Figure 3 shows the

XRD patterns of the hematite (α-Fe$_2$O$_3$), containing nine distinguishable peaks. All of them can be perfectly indexed to rhombohedral Fe$_2$O$_3$ in terms of the peak positions (JCPDS No.24-0072), with space group R3 (148). Figures 4 (a) and (b) show the SEM images of the α-Fe$_2$O$_3$/TiO$_2$ nanotube arrays composite samples. The α-Fe2O3 nanoparticles were homogeneously introduced into the TiO$_2$ nanotube arrays.
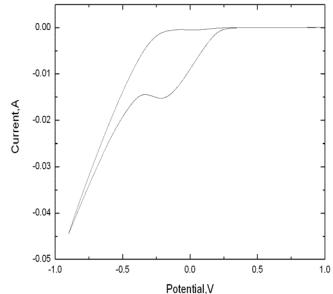
Fig. 2 Cyclic voltammogram in the α-Fe$_2$O$_3$ deposition solution
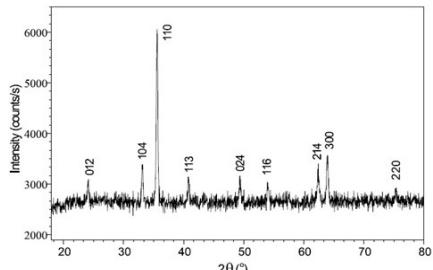

Fig.3 X-ray diffraction pattern of α-Fe$_2$O$_3$

(a)   (b)
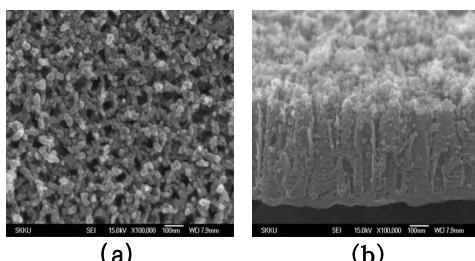
Fig.4 FE-SEM images of α-Fe$_2$O$_3$ doped TiO$_2$ nanotube arrays

3.3 Photoelectrochemical properties

Figure 5 shows the current-potential (I-V) curves of the α-Fe$_2$O$_3$ doped TiO$_2$ nanotube arrays in 1 M NaOH solution in the dark and when illuminated by UV-visible light (Xenon lamp, 100 mW /cm^2, ABET, LS-150-Xe). The I-V responses for the samples obtained in the dark are similar. The photocurrent observed under illumination is a direct measure of the rate of splitting and reflects the number of charge carriers produced from the incident light and their subsequent participation in water oxidation on the photoanode and hydrogen ion reduction on the counter electrode.
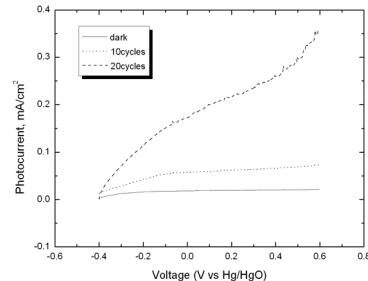

Fig.5 Current-potential (I-V) curves of annealed α-Fe$_2$O$_3$ doped TiO$_2$ nanotube arrays in 1 M NaOH solution in the dark and under illumination (100 mW/cm^2).

The inset of Fig. 5 shows the steady state photocurrent density. The anodic characteristics of the photocurrent indicate that the film exhibits photoactivity with n-type behavior. The main defect type in hematite is oxygen vacancies [21], which are responsible for the n-type behavior by donating electrons to the conduction band. Moreover, the high temperature annealing increases the concentration of oxygen vacancies.

As can be seen, the α-Fe$_2$O$_3$ doped TiO$_2$ nanotube arrays show a much high photocurrent at a higher potential. Among all of the compositions, the α-Fe$_2$O$_3$ doped sample subjected to 20 cycles exhibits the highest performance. The hematite in the TiO$_2$ nanotube arrays may act in two ways [22]. First, the α-Fe$_2$O$_3$ generates more electrons excited by visible light due to its relative lower bandgap. The increase in the donor concentration in the case of n-type doping would improve the conductivity and enhance the charge transfer, while decreasing the carrier recombination. Second, the increase in the donor concentration would increase the electric field across the space charge layer, resulting in higher charge separation efficiency.

4. Conclusion

α-Fe$_2$O$_3$ was successfully introduced into TiO$_2$ nanotube arrays by electrochemical deposition followed by high temperature calcination. The results revealed that the α-Fe$_2$O$_3$ coupled TiO$_2$ composite consists of uniform anatase nanotubes with an average tubular diameter of 13nm with homogenously loaded α-Fe$_2$O$_3$ nanoparticles. The absorption edge of the TiO$_2$ nanotube array composite can be extended to the visible region by loading it with α-Fe$_2$O$_3$ nanoparticles. The α-Fe$_2$O$_3$/TiO$_2$ nanotube array composite exhibited an improvement in its efficiency for photoelectrochemical water splitting, due to the

heterojunction formed at the interface of α-Fe$_2$O$_3$ and the TiO$_2$ nanotube arrays, so as to enhance the separation efficiency of the photogenerated electron-hole pairs.

References

[1] Ashokkumar M, 1998, "An overview on semiconductor particulate systems for photoproduction of hydrogen",Int. J. Hydrogen Energy, Vol. 23, Issue 6, pp. 427-438, 1998.

[2] Serpone N, Pelizzetti E, 1989, Photocatalysis: Fundamentals and Applications, New York, Wiley 1989.

[3] Schiavello M, Dordrecht H, 1985, Photoelectrochemistry, Photocatalysis and Photoreactors: Fundamentals and Development, Boston, Kluwer Academic Publishers 1985.

[4] Linsebigler AL, Lu G., Yates JT, 1995, Chem. Rev.,Vol. 95: pp. 735, 1995.

[5] Kim EY, Park JH, Han GY, 2008, "Design of TiO2 nanotube array-based water-splitting reactor for hydrogen generation", J. Power Sources, Vol. 184,pp. 284-287, 2008.

[6] Ou H, Lo S, 2007, "Review of titania nanotubes synthesized via the hydrothermal treatment: Fabrication, modification, and application", Sep Purif Technol Vol. 58, pp. 179-191, 2007.

[7] Kasuga T, Hiramatsu M, Hoson A, Sekino T, Niihara K, 1999, "Titania nanotubes prepared by chemical processing", Adv. Mater. Vol. 11, pp. 1307-1311, 1999.

[8] Du GH, Chen Q, Che RC, Yuan ZY, Peng LM, 2001, "Preparation and structure analysis of titanium oxide nanotubes", Appl. Phys. Lett. Vol. 79, pp. 3702-3704, 2001.

[9] Chen Q, Zhou WZ, Du G.H, Peng LM, 2002, "Trititanate Nanotubes Made via a Single Alkali Treatment", Adv. Mater. Vol. 14: pp. 1208-1211, 2002.

[10] Chen Q, Du G.H, Zhang S, Peng LM, 2002, "The structure of trititanate nanotubes", Acta Cryst. B Vol. 58: pp. 587-593, 2002.

[11] Tsai CC, Teng H, 2004, "Regulation of the Physical Characteristics of Titania Nanotube Aggregates Synthesized from Hydrothermal Treatment", Chem. Mater., Vol. 16, pp. 4352-4358, 2004.

[12] Tsai CC, Nian JN, Teng H, 2006, "Mesoporous nanotube aggregates obtained from hydrothermally treating TiO2 with NaOH", Appl. Surf. Sci. Vol. 253: pp. 1898-1902, 2006.

[13] Chen S, Paulose M, Ruan C, Mor GK, Varghese OK, Kouzoudis D et al, 2006, "Electrochemically synthesized CdS nanoparticle-modified TiO2 nanotube-array photoelectrodes: Preparation, characterization, and application to photoelectrochemical cells", J. Photochem. Photobio. A: Chemistry Vol. 177, pp. 177-184, 2006.

[14] Zhang YJ, Yan W, Wu YP, Wang ZH, 2008, "Synthesis of TiO2 nanotubes coupled with CdS nanoparticles and production of hydrogen by photocatalytic water decomposition", Materials Letters Vol. 62, pp. 3846-3848, 2008.

[15] Wang N, Li X, Wang Y, Hou Y, Zou X, Chen G, 2008, "Synthesis of ZnO/TiO2 nanotube composite film by a two-step route", Materials Letters Vol. 62, pp. 3691-3693, 2008.

[16] Brahimi R, Bessekhouad Y, Bouguelia A, Trari M, 2007, "CuAlO2/TiO2heterojunction applied to visible light H2 production", Journal of Photochemistry and Photobiology A: Chemistry Vol. 186, pp. 242-247, 2007.

[17] Parkhutik VP, Shershulsky VI, 1992, "Theoretical Modeling of Porous. Oxide Growth on Aluminium", J. Phys. D: Appl. Phys. Vol. 25, pp. 1258-1263, 1992.

[18] Pakes A, Thompson GE, Skeldon P, Morgan PC, 2003, "Development of porous anodic films on 2014-T4 aluminium alloy in tetraborate electrolyte", Corros. Sci. Vol. 45, pp. 1275-1287, 2003.

[19] Siejka J, Ortega C, 1977, "An O18 study of field-assisted pore formation in compact anodic oxide films on aluminium", J. Electrochem.Soc. Vol. 124, pp. 883-891, 1977.

[20] Thompson GE, 1997, "Porous anodic alumina: fabrication, characterization and applications", Thin Solid Films Vol. 297, pp. 192-201, 1997.

[21] Lindgren T, Wang H, Beermann N, Vayssieres L, Hagfeldt A, S.-E. Lindquist, 2002, "Aqueous photoelectrochemistry of hematite nanorod array", Sol. Energy Mater. Sol. Cells Vol. 71: pp. 231-243, 2002.

[22] Schrebler R, Bello K, Vera F, Cury P, Munoz E, RIO RD et al, 2007, "An Electrochemical Deposition Route for Obtaining alpha-Fe2O3 Thin Films II. EQCM Study and Semiconductor Properties", Electrochemical and solid-state lettersVol. 10, pp. D95-D99, 2007.